26th EPS Conf. on Contr. Fusion and Plasma Physics, Maastricht, 14 - 18 June 1999 ECA Vol.23J (1999) 105 - 108

Reversed magnetic shear operation with ICRF minority heating on Tore Supra

G.T. Hoang, G. Antar, T. Aniel, V. Basiuk, A. Bécoulet, C. Bourdelle, R.V. Budny, P. Devynck, X. Garbet, J. Lasalle, G. Martin, and F. Saint-Laurent
Association Euratom-CEA sur la Fusion Contrôlée
CEA Cadarache, 13108 Saint-Paul-lez-Durance, France

Reversed magnetic shear (RS) plasma configuration with internal transport barrier (ITB) is one of the most promising ways to achieve high performance regimes, as proved in many tokamaks (TFTR [1], DIII-D [2], JT-60U [3], and JET [4]). Tore Supra has demonstrated the sustainment of a steady-state RS plasma with non-inductive current drive by lower hybrid waves (LHCD) only. RS plasmas with an improved confinement have been maintained for up to 1 minute [5]. Nowadays, one of the most attractive schemes of operation consists in applying the auxiliary heating, usually neutral beam injection, very early in the discharge during the plasma current (I_p) ramp-up.

This paper reports a scenario recently investigated in Tore Supra for high density and high plasma current (I_p) operation, which allows us to use the ion cyclotron resonance frequency (ICRF) minority heating only for the ITB formation. The main aim is to preform a hollow current density profile by minimizing the edge resistive skin depth during the rapid I_p ramp-up, i.e. efficient freezing of the resistive current diffusion. The skin depth is defined as $\delta \approx (2\eta / \omega_{ramp})^{0.5}$. η and ω_{ramp} are, respectively, the plasma resistivity and the current ramp-up rate ($\omega_{ramp} \approx (1/I_p)*(dI_p/dt)$). To minimize δ we must increase ω_{ramp} and/or reduce η (by increasing the electron temperature by additional heating). In our experiments , the ICRF heating is not necessary for the formation of the hollow current profile as in the previously mentioned experiments. The ICRF power is applied after the RS formation by optimization of ω_{ramp} during the ramp-up. The scenario consists in setting a low I_p flat top phase ($\leq$ 0.4 MA) long enough (several seconds) to reach a steady-state (Fig.1). The plasma current is then rapidly ramped up (to 1.2 MA). The first stationary flat top phase is required for i) a high density operation, up to $7x10^{19}$ m^{-3} (0.65 x Greenwald limit) ii) a rapid I_p ramp-up (dI_p/dt up to 1.6 MA/s): the stationary plasma pressure is large enough to avoid the onset of MHD activity. Another advantage of such a scenario is to obtain a stationary density high enough for coupling a large amount of ICRF power. For Tore Supra circular plasmas, the time required for reaching such density, by gas puffing during the start-up phase, is however much larger than the resistive time scale (a few hundreds of ms).

In Figure 1, the evolutions of ω_{ramp}, δ, and self-inductance (l_i) when I_p is ramped-up from 0.4 MA to 1.2 MA, without additional heating, are shown for two scenarios. In the case 1, I_p is raised at the rate dI_p/dt = 1.6 MA/s, after a 0.4 MA stationary phase of 8.5 s. For case 2, I_p is ramped in the early time of the discharge at dI_p/dt = 0.35 MA/s. In the first case, high value of ω_{ramp}, induces a thin skin depth at the edge (normalized radius r/a = 0.7), which is about 0.2 m (minor radius a = 0.75 m) compared to the value of about 0.5 m in the second case. As a consequence, a drop of l_i to a low value around 0.7 is observed, characterizing a broadening of the current profile. Conversely, l_i increases to the value of 1.2 in the case 2, which indicates a peaked profile. In figure 2, the evolution of the current density is plotted at various radii. The current density profiles are obtained by an Abel inversion of the Faraday rotation angles measured from polarimetry diagnostic. Case 1 shows that the central current density is effectively frozen when I_p increases from 0.6 MA to 1.2 MA. The added resistive current (0.6MA) is mostly accumulated in the region $0.5 < r/a < 1$ (Fig. 4). The value at mid-radius increases from 0.5 MA/m^2 to 1.2 MA/m^2 and becomes higher than the central value which is almost constant (less than 1 MA/m^2). In the case 2, an opposite behaviour of the current diffusion is observed. The resistive current rapidly diffuses to the core region: the central value rises from 0.6 MA/m^2 to 1.8 MA/m^2, exceeding the mid-radius value which weakly increases.

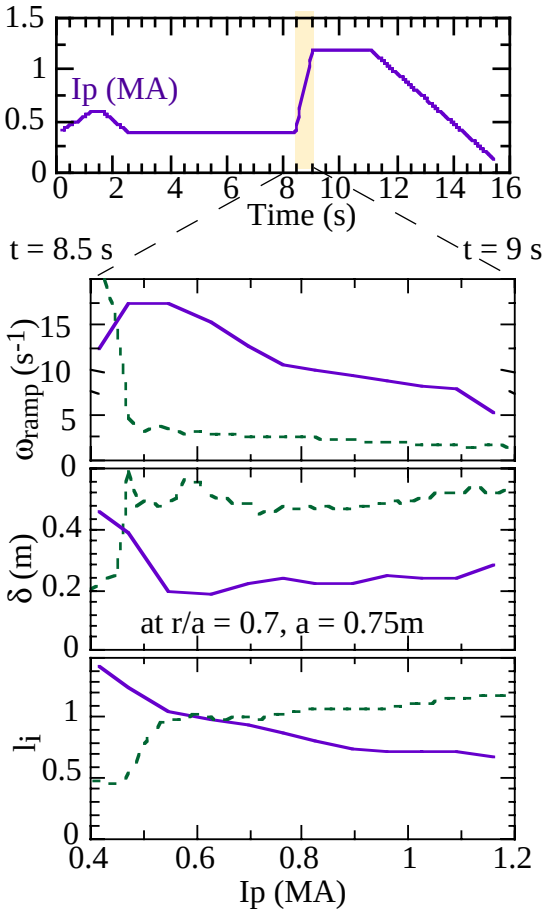

Figure 1: Ramp-up rate, skin depth (at r/a = 0.7), and self-inductance versus total current for two scenarios. Case 1 (full): ramp-up between 8.5 s and 9 s, after a steady-state I_p = 0.4MA. Case 2 (dashed): start-up phase between 0.1s and 2.5s.

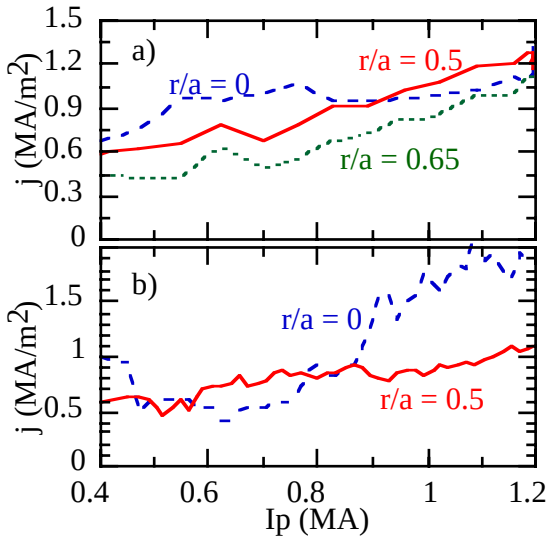

Figure 2: Evolution of current density at various radii during the plasma current ramp-up from 0.4 MA to 1.2 MA for shots in Fig 1 (a: case 1, b: case 2, i.e. start-up phase).

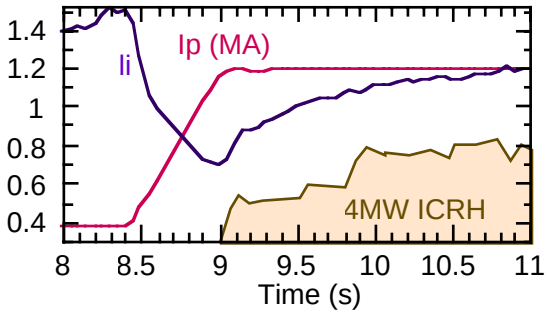

Figure 3: ICRF H-minority heating discharge with preformed hollow current profile.

Figure 3 illustrates a typical discharge (#TS25196) carried out at the central density of $6.5 \times 10^{19} m^{-3}$. After a stationary current plateau of 0.4 MA / 8.5s, I_p is ramped to 1.2 MA. An ICRF power of 4 MW is applied at the end of the I_p ramp-up (t = 9 s), after the formation of the hollow profile. The preformed RS configuration (at t = 8.7 s, with central value of safety factor, q(0), between 2.5 and 3) is transiently maintained for about 0.2 s, from t = 9 s to t = 9.2 s, when the ICRF power is applied. The time evolution of the current density profile is shown in Fig. 4. Within the error bars the minimum value of q (slightly higher than 2) is found to be located between r/a = 0.5 and r/a = 0.6. This transient hollow profile relaxes to a flat profile. In spite of a dominant on-axis electron heating the flat profile remains until the end of the I_p plateau (t = 11 s). At the time t = 10 s, an improved confinement transition is observed (Fig. 5). Normalized beta increases until the end of the current plateau, t = 11 s reaching the value of 0.7, while the total power is kept constant and the gas fueling is switched-off at t = 9 s. The total energy is found higher than the ITER L-mode prediction [6] by about 40% (confinement time τ_E = 130 ms compared to 95 ms of a reference L-mode shot, and τ_E^{ITER} = 90 ms). Also, the electron energy exceeds the Rebut-Lallia-Watkins L-mode scaling, which usually reproduces the Tore Supra L-mode [7], by a factor of 1.4. Ion temperature profiles are not available in our experiments, but the same enhancement factor in both total and electron energies suggests that the ion confinement is also improved. A clear transport barrier is observed inside the region r/a = 0.6 in the electron channel. Electron temperature and density profiles become more peaked inside the low shear region. Figure 6 shows the electron pressure

and magnetic shear profiles of shot #TS25196. One can see that the electron pressure gradient significantly increases within the region r/a < 0.6 where the magnetic shear is lower than 0.3 (usually 0.7 in the L-mode).

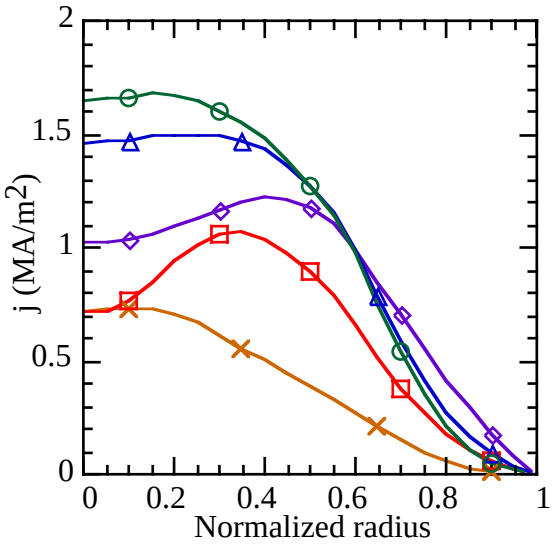

Figure 4: Current profiles of discharge #TS25196, in Fig 3, before (at t = 8.2 s: cross, and t = 8.7 s: square) and after ICRF application (at t = 9.1 s: diamond, t = 9.8 s: triangle, t = 10.8 s: circle).

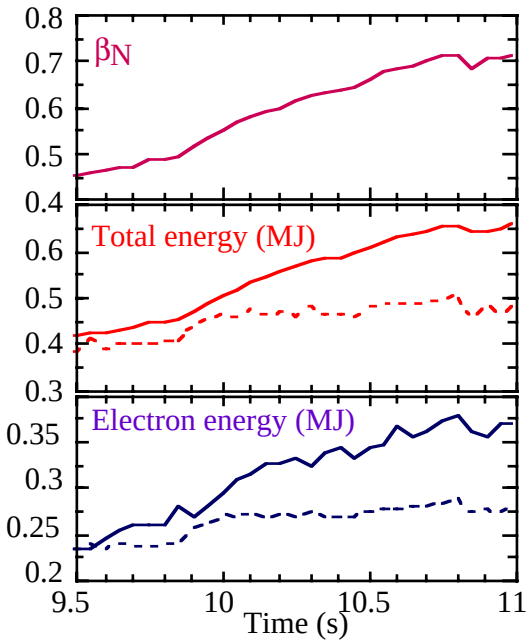

Figure 5: Time evolution normalized beta (β_N), total and electron energies (dashed curves correspond to the ITER L-mode scaling for total energy and the electron Rebut-Lallia-Watkins L-mode scaling).

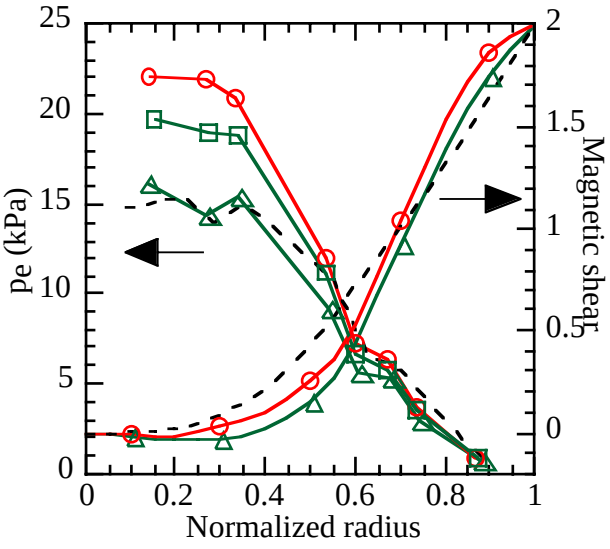

Figure 6: Electron pressure and magnetic shear profiles of shot #TS25196 in Fig 3, at t = 9.8s (triangle, 2MW), t = 10.2s (square, 4MW), and t = 10.8s (circle, 4MW). Dashed curve corresponds to the reference L-mode shot.

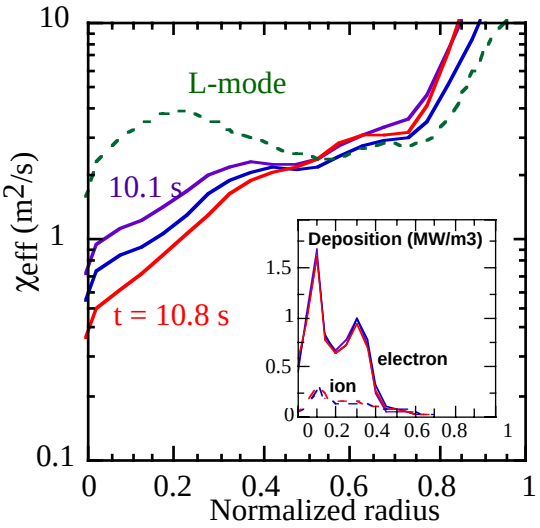

Figure 7: Comparison of 1-Fluid effective diffusivity (#TS25196) with a reference L-mode.

A 1-fluid transport analysis shows that the effective heat diffusivity (χ_{eff}) is reduced by a factor of 3-4 from the L-mode value in the flat q profile region. Figure 7 shows the profile of χ_{eff} of shot TS25196 for three time slices during the improved confinement phase: 0.1 s, 0.4 s,

and 0.8 s after the transition (t = 10.1 s, 10.5 s, 10.8 s) together with a reference L-mode shot. For this analysis, the ICRF power deposition is computed by the PION code [8]. The calculation gives a power coupled to the electrons of about 80% of the total injected power with an unchanged deposition profile during the improvement phase.

A stability analysis with a gyrofluid code indicates that the stabilizing effect in the core region is mainly due to the magnetic shear reversal during the transient preformed current phase. The radial profile of the maximum linear growth rate (γ^{max}), calculated at t = 9.1 s (hollow profile), is plotted in Fig. 8. γ^{max}, computed by assuming a monotonic profile, is also reported in this figure. This suggests that the negative magnetic shear reduces γ^{max} to the level of the ExB shear stabilizing effect ($\gamma_E = \frac{d}{dr}\left(\frac{E_r}{B}\right)$, E_r being the neoclassical value including the ripple effect). In the plateau with ICRF heating, this effect of magnetic shear (flat profile) becomes weaker, and a larger stabilizing ExB shear takes place.

For this experiment, the density fluctuations are measured by heterodyne CO_2 laser scattering diagnostic for k = 8 cm^{-1}. Preliminary results indicate that the turbulence intensity, during the current ramp-up phase when the hollow current profile is formed, is significantly reduced and remains at a low level during the ICRF power application. Figure 9 shows the normalized rms signal ($(\delta n/n)^2$) as a function of the product $n_e.\nabla T_e$. It decreases with increasing $n_e.\nabla T_e$, while an opposite variation is usually observed in the L-mode (Fig.9).

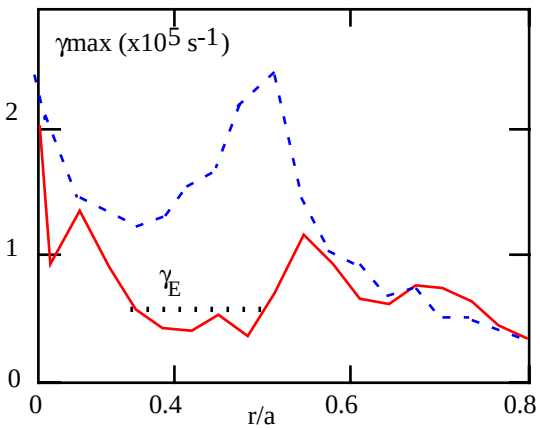

Figure 8: Radial profile of linear growth rate for shot #TS25196, at t = 9.1 s. Dashed curve: calculation assuming a monotonic q profile. Stabilizing ExB shear is from neoclassical calculation with the ripple effect.

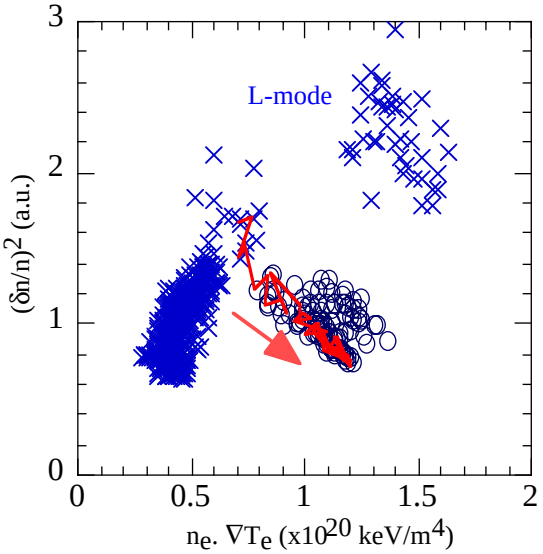

Figure 9: Statistical analysis of density fluctuation versus $n_e.\nabla T_e$. Cross: L-mode. Circle: shots of scenario described in this paper, the full line illustrates the trajectory of one of these shots.

[1] Levinton, F.M., et al., Phys. Rev. Lett. **75** 4417.
[2] Strait, E.J., et al., Phys. Rev. Lett. **75** 4421.
[3] Ishida, S., et al., Phys. Rev. Lett. **79** 3917.
[4] Gormezano, C., et al., Phys. Rev. Lett. **50** 5544.
[5] Equipe Tore Supra Plasma Phys. Control. Fusion **38** (1996) A251.
[6] Kaye, S.M, et al., Nuclear Fusion **37** (1997) 1303.
[7] Hoang, G.T., et al., Nucl. Fusion, **34** (1994) 75.
[8] Eriksson, L.-G., et al., Nucl. Fusion **33** (1993) 1037.
[9] Hoang, G.T., et al., Nucl. Fusion, **38** (1998) 117.